







BRIEF COMMUNICATION

GGPS1-associated muscular dystrophy with and without hearing loss

Rauan Kaiyrzhanov¹ , Luke Perry^{2,3} , Clarissa Rocca¹ , Maha S. Zaki⁴, Heba Hosny^{5,6}, Cristiane Araujo Martins Moreno⁷, Rahul Phadke², Irina Zaharieva² , Clara Camelo Gontijo⁷, Christian Beetz⁶, Veronica Pini², Mojtaba Movahedinia⁸, Edmar Zanoteli⁷, Stephanie DiTroia⁹, Sandrine Vuillaumier-Barrot¹⁰, Arnaud Isapof¹¹, Mohammad Yahya Vahidi Mehrjardi¹², Nasrin Ghasemi¹³, Anna Sarkozy^{2,3}, Francesco Muntoni^{2,3,14}, Sandra Whalen¹⁵, Barbara Vona^{16,17} , Henry Houlden¹ & Reza Maroofian¹ 

¹Department of Neuromuscular Disorders, UCL Queen Square Institute of Neurology, London, WC1N 3BG, UK

²The Dubowitz Neuromuscular Centre, University College London, Great Ormond Street, Institute of Child Health and MRC Centre for Neuromuscular Diseases, Neurosciences Unit, Great Ormond Street Hospital, London, UK

³MRC UCL International Centre for Genomic Medicine in Neuromuscular Diseases (ICGNMD), London, UK

⁴Clinical Genetics Department, Human Genetics and Genome Research Division, National Research Centre, 12622, Cairo, Egypt

⁵National Institute of Neuromotor System, Cairo, Egypt

⁶Diagnostic Department, Centogene GmbH, 18055, Rostock, Germany

⁷Department of Neurology, School of Medicine of Universidade de Sao Paulo, Sao Paulo, Brazil

⁸Children Growth Disorder Research Center, Shahid Sadoughi University of Medical Sciences, Yazd, Iran

⁹Program in Medical and Population Genetics and Center for Mendelian Genomics, Broad Institute of MIT and Harvard, Cambridge, Massachusetts, USA

¹⁰Service de Biochimie et génétique, APHP, Hôpital Bichat-Claude Bernard, 75018, Paris, France

¹¹Service de neuropédiatrie, APHP, Sorbonne Université, Hôpital Armand Trousseau, 75012, Paris, France

¹²Medical Genetics Research Center, Shahid Sadoughi University of Medical Sciences, Yazd, Iran

¹³Abortion Research Centre, Yazd Reproductive Sciences Institute, Shahid Sadoughi University of Medical Sciences, 8916978477, Yazd, Iran

¹⁴NIHR Great Ormond Street Hospital Biomedical Research Centre, Great Ormond Street Institute of Child Health, University College London, London, UK

¹⁵UF de Génétique Clinique, Centre de Référence Maladies Rares Anomalies du Développement et Syndromes Malformatifs, AP-HP. Sorbonne Université, Hôpital Armand Trousseau, 75012, Paris, France

¹⁶Institute of Human Genetics, University Medical Center Göttingen, Göttingen, Germany

¹⁷Institute for Auditory Neuroscience and Inner Ear Lab, University Medical Center Göttingen, Göttingen, Germany

Correspondence

Reza Maroofian, Department of Neuromuscular Disorders, UCL Queen Square Institute of Neurology, London WC1N 3BG, UK. Tel: +44 (0)2034484069; Fax: +44 (0) 20 7278 5616; E-mail: r.maroofian@ucl.ac.uk

Funding Information

This research was funded in part, by the Wellcome Trust [WT093205MA, WT104033AIA and the Synaptopathies Strategic Award, 165908]. This study was funded by the Medical Research Council (MR/S01165X/1, MR/S005021/1, G0601943). This research was conducted as part of the Queen Square Genomics group at University College London, supported by the National Institute for Health Research University College London Hospitals Biomedical Research Centre. This work was supported by funding from the German Research Foundation through the Collaborative Research Center 889 and the Multiscale

Abstract

Ultra-rare biallelic pathogenic variants in geranylgeranyl diphosphate synthase 1 (*GGPS1*) have recently been associated with muscular dystrophy/hearing loss/ovarian insufficiency syndrome. Here, we describe 11 affected individuals from four unpublished families with ultra-rare missense variants in *GGPS1* and provide follow-up details from a previously reported family. Our cohort replicated most of the previously described clinical features of *GGPS1* deficiency; however, hearing loss was present in only 46% of the individuals. This report consolidates the disease-causing role of biallelic variants in *GGPS1* and demonstrates that hearing loss and ovarian insufficiency might be a variable feature of the *GGPS1*-associated muscular dystrophy.

Bioimaging Cluster of Excellence (MBExC) (BV). L.P. was supported by an MRC strategic award to establish an International Centre for Genomic Medicine in Neuromuscular Diseases (ICGNMD) MR/S005021/1. We acknowledge the support of the MRC Centre for Neuromuscular Disease Biobank and HSS England National Specialist Diagnostic and Advisory Service for Congenital Muscular Dystrophies and Congenital Myopathies. The research leading to these results has received funding from the Muscular Dystrophy Campaign grant "Understanding the function of novel congenital muscular dystrophies and congenital myopathies genes" (Grant reference number: 18GRO-PG24-0271) and from the European Union's Horizon 2020 research and innovation programme grant "SOLVE-RD: solving the unresolved Rare Diseases" (grant agreement No 779257). Sequencing and analysis of Family 3 were provided by the Broad Institute of MIT and Harvard Center for Mendelian Genomics and was funded by the National Human Genome Research Institute, the National Eye Institute, and the National Heart, Lung and Blood Institute grant UM1 HG008900, and in part by National Human Genome Research Institute grants U01 HG0011755 and R01 HG009141. For the purpose of open access, the author has applied a CC BY public copyright license to any author accepted manuscript version arising from this submission.

Received: 23 March 2022; Revised: 22 June 2022; Accepted: 3 July 2022

***Annals of Clinical and Translational Neurology* 2022; 9(9): 1465–1474**

doi: 10.1002/acn3.51633

Introduction

Geranylgeranyl diphosphate synthase 1 (*GGPS1*) is a member of the prenyltransferase family and encodes a protein with geranylgeranyl diphosphate (GGPP) synthase activity. The enzyme catalyzes the synthesis of GGPP from farnesyl diphosphate and isopentenyl diphosphate. GGPP is an important molecule responsible for the C20-prenylation of proteins. Prenylation provides proteins with a hydrophobic C terminus, the consequence of which is a greatly increased capacity to interact with cellular membranes, which have a high concentration of signaling molecules.^{1,2} Prenylation is particularly important for small guanosine triphosphatases (GTPases) such as

the Rab family, which have crucial roles in vesicular trafficking in mammalian cells.² The roles of prenylated proteins in cells are well conserved across species.¹

While monoallelic variants in *GGPS1* have been identified as a risk factor for atypical femoral bone fractures in females exposed to bisphosphonates, ultra-rare biallelic pathogenic missense variants in *GGPS1* have recently been associated with muscular dystrophy/hearing loss/ovarian insufficiency syndrome.^{2,3} Here, we describe 11 affected individuals from four previously unreported British, Iranian, Egyptian, and Brazilian families harboring ultra-rare missense variants in *GGPS1* and provide follow-up clinical data from the previously reported two Pakistani cases by Tucker et al. (2020).³

Subjects and Methods

Two of the novel families reported here were recruited from Iran and Egypt as part of the SYNAPS project at the Institute of Neurology, University College London (UCL). The third and fourth novel families were identified through a collaboration between Great Ormond Street Institute of Child Health (UCL) and the Center for Mendelian Genomics, Broad Institute, USA and School of Medicine of Universidade de Sao Paulo, respectively. The corresponding author was contacted from Tucker et al. (2020)³ to obtain follow-up details from the reported 2 persons with homozygous *GGPS1* variants. To identify the genetic cause of the disease in the affected individuals, exome sequencing on DNA extracted from probands' leukocytes and variant filtering were performed as described (Table 1 for genetic methods). To assess *Ggps1* RNA expression in the mouse cochlear epithelium at various stages (embryonic (E) 14, and postnatal (P) 1 and P7), publicly available single cell RNA-seq data were visualized using the gene expression analysis resource (gEAR).⁷ The publicly available Mouse Cell Atlas, generated as previously described,⁸ includes single-cell RNA sequencing data used to visualize global expression of *Ggps1* in the female E14.5 gonad (version 2.0 with >520,000 cells from over 10 mouse tissues grouped into 95 major clusters) and neonatal skeletal muscle excised from the leg (version 1.0 with >400,000 cells from over 10 mouse tissues grouped into 104 major clusters). Clusters showing expression (red) are marked in black numbers representing the cluster code defined on the Mouse Cell Atlas.⁸ The study was approved by the ethics Institutional Review Board of UCL and additional local ethics committees of the participating centres. Informed consent was obtained from all families.

Results

The affected individuals are six males and seven females, all of whom were born at full term, with all but two (P10 and P11) conceived from consanguineous unions (Fig. 1A). Eleven affected individuals are alive with a mean current age of 10 ± 6 years (range 4–24), and two individuals died at the ages of 11 months and 30 years old due to respiratory insufficiency and choking, respectively. Antenatal history was unremarkable in all but 3/13 persons who displayed decreased foetal movements.

Tables 1 and 2, Table S1, and Videos S1–S6 provide details on the clinical phenotype of the present cohort. The disease onset ranged from prenatal (3/13) to preschooler age (mean age 16 ± 9.4 months, range 4–36). Delayed motor milestones (10/13), weak cry (3/13) and muscle weakness (3/13) were the first presenting symptoms. Mean ages were 9.7 ± 1.7 months for sitting,

1.7 ± 0.3 years for walking, and 9.9 ± 2.9 months for first words. Proximal or generalized muscle weakness (12/13) with the mean onset age of 2.7 ± 2.7 years (range 0.6–11), respiratory insufficiency (8/13) requiring non-invasive ventilation (6/13) and tracheostomy (2/13), joint contractures (7/12), congenital or infantile-onset bilateral severe sensorineural hearing loss (6/13) (only present in Families 1, 3, 4, and 5, while in the rest of the persons the absence of sensorineural hearing loss was clinically and objectively confirmed), and gastrointestinal issues (4/13) were among the commonly reported symptoms throughout the disease course (Tables 1 and 2). The age of onset for respiratory insufficiency in the affected individuals ranged between 7 months to 20 years old. Only one female person has reached puberty, and at 30 years old, she does not have clinical signs of primary ovarian insufficiency, while follicle-stimulating hormone levels were reported to be high in P11, aged 12 years old. Six affected individuals lost ambulation at the mean age of 8.1 ± 4.7 years. Ninety-two percent (12/13) of individuals displayed slow rates of disease progression. One person (P10) demonstrated improvement in motor abilities and dysphagia symptoms in childhood. Older individuals in our series tended to have a more severe phenotype reflecting the progressive nature of the disease in most instances.

On the most recent examination, a mean age of the affected individuals was 11.5 ± 7.8 years (range 4.6–29). They had normal cognition (0/13) with short stature (8/13) and progressive scoliosis (7/11). Neuromuscular examination revealed hypotonia (10/13), proximal or generalized muscle weakness (12/13), and muscular atrophy (12/12) accompanied with stiffness (6/12), calf hypertrophy (4/12), hyporeflexia/areflexia (12/12), and myalgia (6/10). Gait was waddling in 4/11 and broad-based in 2/11 persons (Tables 1 and 2). Electromyography findings were compatible with myopathy in 8/13 and elevated creatinine kinase (CK) (1594–27000 U/L) was registered in 10/10 individuals. Lower limb muscle magnetic resonance imaging in Family 3 (P10), performed at the age of 8 months old, showed generalized muscle atrophy without fatty infiltration (Fig. 1E). Muscle biopsy from the quadriceps at age 8 months old in P10 showed type 1 fiber predominance and central nucleation with Z line streaming and minicores evident on electron microscopy (Fig. 1D, I–IV). Muscle biopsy from the biceps in Family 4 (P11) showed fatty infiltration with mitochondrial changes (Fig. 1D, V–VII), whereas in Family 5 it showed a dystrophic pattern.

On exome sequencing, an ultra-rare homozygous missense variant in exon 4 of *GGPS1* c.269A > G, p.(Asn90Ser) (NM_004837.4) residing within a 9.77 Mb region of homozygosity was identified in Family 1 (Fig. 1A–C, Figure S1). The p.(Asn90Ser) variant is located in a highly

Table 1. Clinical features of the affected individuals with biallelic GGPS1 variants.

Variant details	Person	Family 1 P1-P3	Family 2 P4-P9	Family 3 P10	Family 4 P11	Family 5 (from Tucker et al., 2020) P12, P13	Foley et al. 2020 (11 p ersons/6 families)	Tucker et al. 2020 (4 persons/2 families)
Variant type		Homozygous	Homozygous	Compound heterozygous	Homozygous	Homozygous	Homozygous/compound heterozygous	Homozygous
Variant at the cDNA level (NM_004837.4)		c.269A > G	c.439A > G	c.196A > C and c.545 T > C	c.770 T > G	c.269A > G	(c.860A > G;865C > G), (c.127C > T; 865C > G), c.866G > A, c.854 T > G	c.782G > A, c.269A > G
Variant at the protein level		p.(Asn90Ser)	p.(Met147Val)	p.(Ile66Leu) and p.(Leu182Pro)	p.(Phe257Cys)	p.(Asn90Ser)	[p.(Tyr259Cys); p.(Arg261Gly)], [p.(Pro155Ser); p.(Arg261Gly)], p.(Arg261His), p.(Phe257Cys)	p.(Arg261His), p.(Asn90Ser)
Methods		Makrythanasis et al. ⁴	Makrythanasis et al. ⁴	Pais et al. 2022, ⁵ Natera- de Benito et al. ⁶	Foley et al. 2020 ²	Tucker et al. 2020 ³	Foley et al. 2020 ²	Tucker et al. 2020 ³
Maximum allele frequency in variant databases*		<0.000001	<0.000001	Absent	Absent	<0.000001	<0.0001 to <0.000001	<0.00001
ACMG		Likely pathogenic PS4, PP1 (moderate), PM2, PP3	Likely pathogenic PS4, PP1 (moderate), PM2, PP3	VUS (PM2, PP3, PP4)	VUS (PM2, PP3)	Likely pathogenic PS4, PP1 (moderate), PM2, PP3	Likely Pathogenic	Likely Pathogenic
Sex		3F	5 M, F	F	F	1 M, 1F	F - 6; M - 5	F - 3, M - 1
Consanguinity		3+	6+	-	+	2+	1 family-no, 5 families -NA	NA
Current age		11 y.o. (P1), 11 m.o. (Deceased) (P2), 8 y.o. (P3)	23.5 y.o., 4 y 8 m.o., 5 y 7 m.o., 4 y.o., 5 y.o., 30 y.o. (Deceased)	8 y.o.	12 y	20 y.o., 8.5 y.o.	29,22,46,45,44,14,21,22,11,8 (y.o.)	36,39,7 (y.o.)
Age of death		P2-11 m.o.	30 y.o. (P9)	Alive	Alive	2 Alive	NA	Alive
Type of progression		Slow	6 Slow	Slow	Slow	Moderate** (P12), Slow*** (P13)	Slow	Slow (1)
Failure to thrive		2+, 1NA(P2)	6-	-	-	8+	8+	NA
Sensorineural hearing loss		3+	6-	+	+	10+, 1-	10+, 1-	3+, 1-
Progressive muscle weakness, onset age		1.5 y.o. (P1), NA (P2), 1.5 y.o. (P3)	4 y.o., 2 y.o., 1.2 y.o., 1.5 y.o., 2 y.o., 3 y.o.	7 m.o.	18 m	11 y.o.*** (P12), -** (P13)	4+, less severe weakness 7	Mild (3), Severe (1)
Joint contractures		2+, 1NA (P2)	2+, 4-	-	+	4+	4+	NA
Respiratory insufficiency, age of onset		+13 m.o. (P1) +8 m.o. (P2) +, 15 m.o. (P3)	2+ (20 y.o.-P9), 4-	+7 m.o.	+10 y.o.	8+, 1NA	8+, 1NA	1+
Non-invasive ventilation		3+	1+, 5-	+	-	4+	4+	2+
POI		3NA	2 na	NA	+	na (P12), - (P13)	3+, 3 uncertain to age	2+
Cardiac involvement		2-, 1NA(P2)	1-	-	-	-** (2)	-	NA
Loss of ambulation (age)		7 y.o. (P1, P3), NA(P2)	2+ (18 y.o. and 17 y.o.) 4-	-	9 y.o.	11 y.o.* (P12), -*(P13)	5+, 11 yo, 13 yo, 15, 12, 11	NA

(Continued)

Table 1 Continued.

	Person	Family 1 P1–P3	Family 2 P4–P9	Family 3 P10	Family 4 P11	Family 5 (from Tucker P12, P13)	Foley et al. 2020 (11 p ersons/6 families)	Tucker et al. 2020 (4 persons/2 families)
Development	Age of sitting	1 y.o.(P1), NA (P1, P3)	1 y.o. (P4, P5) 8 m.o. (P6–P8), 9 m.o. (P9)	11 m.o.	8 m	NA(P12), 9 m.o.*(P13)	NA	NA
	Age of walking	2.5 y.o. (P1, P3), NA(P2)	2.2 y.o., 1.7 y.o., 2 y.o., 1.4 y.o., 2.1, 2 y.o.	2 y.o.	18 m	24 m.o.**; 18 m.o.**	18 m.o.	NA
	Age of first words	8 m.o. (P1, P3), 9 m.o. (P2)	8 m.o., 9 m.o. (P5, P6, P8, P9), 1 y.o.		18 m	Normal (P12), Few words* (P13)	NA	NA
Physical examination	Age at last examination	11 y.o. (P1), 9 y.o. (P3), NA (P2)	23.5 y.o., 4.6 y.o., 5.5 y.o., 4 y.o., 5 y.o., 29 y.o.	7 y.o.	12 y	20 y.o., 8 y.o.	28, 26 m.o.	NA
	Progressive scoliosis	–(P1), NA(P2), +(P3)	3+, 3–	+	+	+**, NA (P13)	8+	NA
	Short stature	2+, NA(P2)	4+, 2–	(25th centile for age)	–	+** (2)	NA	NA
Neurological examination	Hypotonia	3–	6+	+	+	+** (2)	NA	NA
	Muscle weakness	2+, NA(P2)	6+	+	+	+	+	2+
	Pattern of muscular weakness	3NA	Generalized (2), Proximal (4)	4 limb Proximal/Axial	Axial and proximal	LL > UL** (2)	NA	NA
	Muscle hypertrophy	2–, NA(P2)	4+, 2–	–	–	–** (2)	NA	NA
	Peripheral neuropathy	3–	6–	–	NA	–** NA (P13)	NA	NA
	DTRs	0(P1, P3), NA(P2)	0 (2), ↓ (4)	↓	↓	↓↓** (2)	NA	NA
	Muscular atrophy	2+, NA(P2)	6+	+	+	+** (2)	NA	NA
	Myalgia	2–, NA(P2)	6+	–	NA	NA (P12), –**	NA	2+
	Muscle stiffness	2+, NA(P2)	2+, 4–	–	NA	+** (2)	NA	NA
	Gait	Broad-based (P1, P3), NA(P2)	Non-ambulant (2), Waddling gait (3), Normal gait (1)	Unsteady	Non-ambulant	NA (P12), Waddling gait*	Non-ambulant (5), NA (6)	NA
Details on Hearing loss	The age of onset	11 m.o.(P1), 6 m.o. (P2, P3)	6 Intact	Normal new-born hearing screen. Hearing loss detected at 4 years	Childhood	Intact (P12), From birth (P13)	From neonatal to childhood	3+, Childhood
	The type of hearing loss	3 SNHL	6–	SNHL	SNHL	–(P12), SNHL (P13)	SNHL	SNHL (3)
	Laterality	Bilateral (P1, P3), NA(P2)	6–	Bilateral	Bilateral	Bilateral (P13)	Bilateral	Bilateral (3)
	Degree	Severe (P1, P3), NA(P2)	6–	Severe	Severe	80 dB ** (P13)	NA	NA
Investigations	Elevated CK (age)	3 NA	6+	+7 m.o 1594 UL, 4 y.o 5490 UL/L	+19 m	2+**	9+	NA
	FSH	3 NA	na (5), NA (1)	NA	High	2 NA	88.2 IU/L, 50.3 IU/L, 53.2 IU/L	60 IU/L, 35.8 IU/L
	EMG	3 Normal	Myopathic changes (6)	Myopathic (8 m.o)	NA	2 Normal**	NA	NA
	Muscle biopsy/histochemistry	3 NA	6 NA	Type 1 fiber predominance, central nuclei, Z line streaming, mini-cores.	Fatty infiltration and mitochondrial changes	2 Dystrophic pattern **	9+, dystrophic, with evidence of degeneration and regeneration	NA
	Muscle MRI	3 NA	6 NA	(8 m.o) generalized muscle atrophy without fatty infiltration.	NA	2 NA	3+, fatty infiltration consistent with an underlying muscular dystrophy.	NA

P, person; NA, not available; na, not applicable; y.o., years old; m.o., months old; SNHL, sensorineural hearing loss; LL, lower limbs; UL, upper limbs; POI, primary ovarian insufficiency; FSG, follicle-stimulating hormone; EMG, electromyography; MRI, magnetic resonance tomography; m, male; f, female; CK, creatine kinase; DTRs, deep tendon reflexes; dB, decibel.
 *Database checked include: GnomAD v3, gnomAD v2.1.1, TopMED Bravo, UKBiobank, Iranome, GME Varome, In-house Database. The total number of alleles considered was ~1,314,000.
 **New information that was not previously reported by Tucker et al. (2020).

conserved GGPS1 protein region. The variant is absent in gnomAD and a number of large publicly available databases apart from 2 heterozygous alleles from the Centogene and TOPMed databases, and is predicted to be damaging by multiple in silico tools. (Table S2). The variant segregated with the phenotype within the family (Fig. 1A). Both Family 1 and Family 5 from Tucker et al. (2020) carried the same recurrent homozygous GGPS1 c.269A > G; p.(Asn90Ser) variant. An ultra-rare homozygous missense variant in exon 4 of GGPS1 c.439A > G; p.(Met147Val) (NM_004837.4) residing within a 9 Mb region of homozygosity was identified in Family 2 (Fig. S1). This variant is located in a highly conserved GGPS1 protein region with predicted-damaging scores on various in silico tools (Table S2). The variant segregated with the phenotype within the family (Fig. 1A).

Based on the extremely rare frequency of the identified GGPS1 variants (PS4, PM2), co-segregation in two unrelated families with multiple affected individuals for the GGPS1 c.269A > G; p.(Asn90Ser) variant (PP1 moderate) and segregation in multiple affected family members from different branches for the GGPS1 c.439A > G; p.(Met147Val) variant (PP1 moderate), as well as predicted-deleterious effect from multiple in silico tools, we classified both variants from Family 1 and 2 as likely pathogenic according to the American College of Medical Genetics and Genomics (ACMG) guidelines for the interpretation of sequence variants.⁹

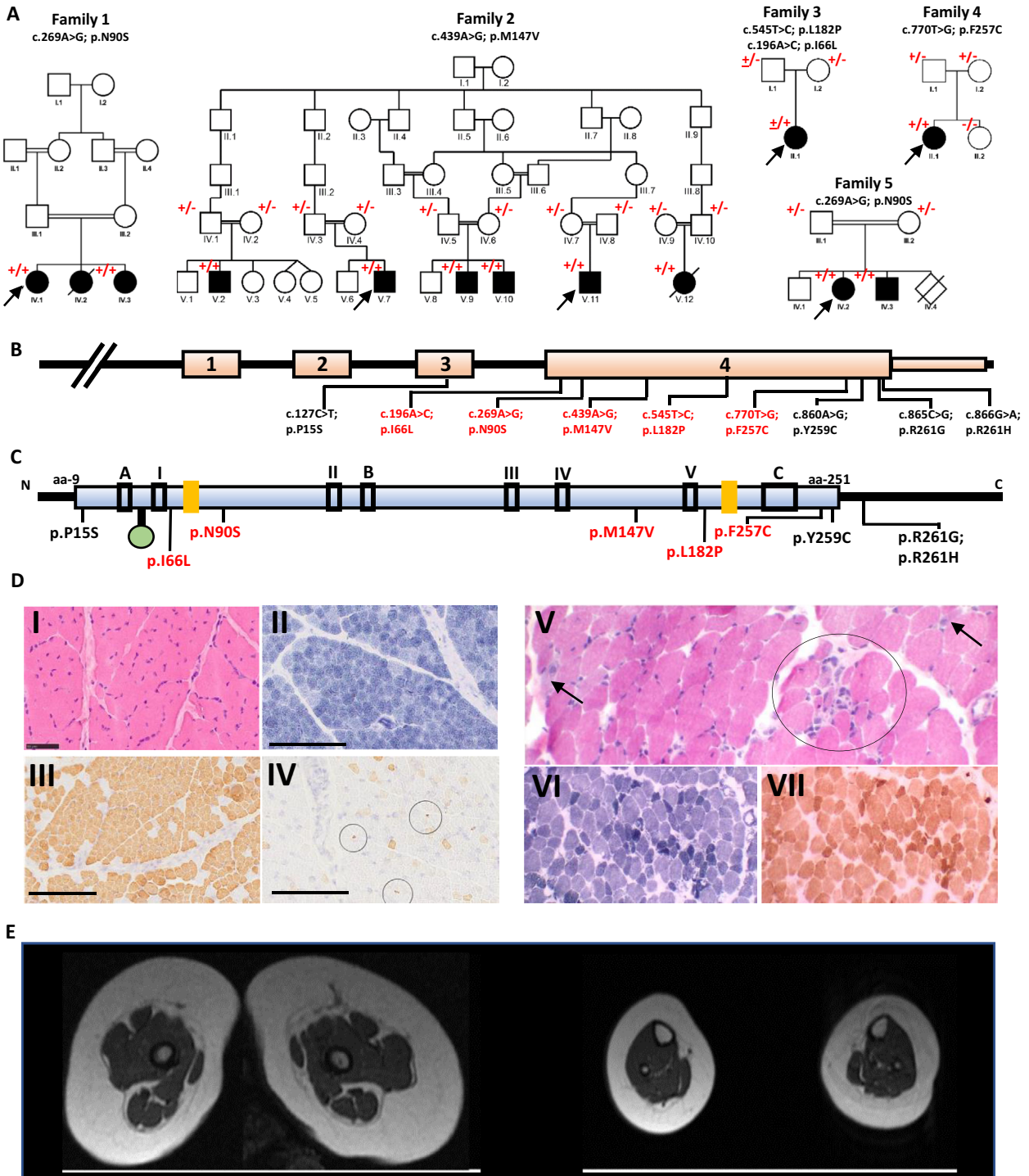
Two ultra-rare missense variants in exon 4 of GGPS1 were identified, in *trans*, in the proband of Family 3 (P10), c.196A > C p.(Ile66Leu) and c.545T > C p.(Leu182Pro) (Fig. 1). Both variants are absent from publicly available databases and are conserved across species (Table S2). The maternally inherited variant, c.196A > C p.(Ile66Leu),

affects the alpha 3 helix of GGPPS whilst the paternally inherited variant affects the alpha 7 helix of the protein. Both implicated residues lie within the enzymes central catalytic barrel. The c.196. A > C p.(Ile66Leu) variant lies between two magnesium ion cofactor ligand bindings sites and the c.545T > C p.(Leu182Pro) variant lies near to the dimethylallyl diphosphate substrate binding sites within the GGPPS protein (Fig. S2). The individual's phenotype was felt to be highly specific for GGPS1 related muscular dystrophy (Table 1). Owing to the rarity of the variants, and lack of further segregation and functional study data, these variants are classified as of uncertain significance according to ACMG guidelines. However, given the affected person's phenotype and proximity of the affected residues to key domains within GGPPS we feel they can be considered disease causing in P10.

An ultra-rare missense variant c.770T > G; p.(Phe257Cys) was identified in Family 4. The variant is absent from all publicly available databases, is conserved across species, and is predicted damaging from a variety of in silico tools (Table S2). The variant segregated with the phenotype within the family (Fig. 1A).

Expression patterns of *Ggps1* in the mouse inner ear, skeletal muscle, and female gonad at different embryonic and postnatal stages were studied using single-cell RNA sequencing. Single-cell RNA sequencing of the cochlear epithelium in the E14, P1, and P7 mouse shows *Ggps1* with a sustained, diffuse expression at these timepoints (Fig. S3). Global view of *Ggps1* expression in the E14.5 female gonad showed clusters most densely in the germ cells and embryonic gonad cells (Fig. S4), whereas neonatal skeletal muscle showed several clusters reflecting comparatively lower expression, for example, in clusters representing stromal cells and chondrocytes (Fig. S5).

Figure 1. Genetic summary, muscle MRI, and muscle histopathology of the affected individuals with biallelic GGPS1 variants. (A) Pedigrees of the five families described in the present report. Square = male; circle = female; black filled symbol = affected individual; white symbols = unaffected individuals; diagonal line = deceased individual. Double lines indicate consanguinity. The allele with the variant is indicated by the + sign. Wild type allele is indicated by the—sign. Inheritance of the compound heterozygous variant in Family 3 is indicated by the underlined + sign. (B) Schematic representation of the GGPS1 gene showing the position of the variants. (C) Schematic diagram indicating the predicted domains and active sites of the GGPS1 protein containing 300 amino acid residues. The blue box represents the polyprenyl synthetase domain. The green circle indicates a magnesium D metal ion binding. Black boxes II, III, and V represent conserved regions that are believed to be involved in ligating the magnesium and the pyrophosphate on the allylic substrate. Box I contains two basic residues involved in IPP pyrophosphate binding. Box IV is the KT sequence containing Thr-152 proposed to be involved in catalysis by stabilizing a carbocation intermediate. Boxes A, B, C are regions thought to be responsible for the hexameric organization of protein.¹² The two yellow boxes are proposed active sites.¹³ (D) Muscle biopsies from affected individuals showed myopathic to dystrophic changes. Family 3 (P10): Quadriceps biopsy performed at 8 months of age (I–IV). Hematoxylin & eosin-stained section shows well-populated fascicles with mild variation in fiber size (I). Staining with NADH-TR shows normal internal architecture and predominance of type I fibers (II). Myosin heavy chain immunohistochemistry shows corresponding predominance of fibers expressing slow myosin heavy chain (III). Aberrant foetal myosin heavy chain expression of varying intensities can be seen in several scattered mature fibers, as well as a population of very small fibers (IV, circles), dispersed across the fascicles. Family 4 (P11): Biceps brachii biopsy performed at 4 years of age (V–VII). Hematoxylin and eosin-stained section shows moderate variation in fiber size (V). There are several scattered (arrow) and clustered (circle) basophilic regenerating fibers (V). Few fibers contain internal nuclei. NADH-TR shows preserved fiber typing, and there are several dark-staining fibers (VI) The cytochrome oxidase stain (COX) also highlights the population of dark staining fibers, but there are no COX-negative fibers (VII). Scale bar: A–D = 50 μm. (E) Muscle MRI of the lower limbs from Family 3 (P10) aged 8 months: Showing generalized atrophy in the absence of muscle fat infiltration.



Discussion

Protein prenylation is an important downstream part of the mevalonate pathway, which is a pivotal process for the synthesis of specialized lipids that play a crucial role

in cellular processes at all levels.^{1,2,10} The mevalonate pathway has recently been suggested to be a novel pathway for muscular dystrophy, hearing loss, and infertility.² Evidence for this comes from the description of 11 individuals from 6 independent families presenting with early

Table 2. Frequency of the clinical features in the *GGPS1* cohorts.

Features	Current report	All reported cases
Decreased foetal movements	3/13	4/14
Birth OFC \leq 25 percentile	6/10	6/10
Manifestation with delayed milestones	10/13	12/15
Slow progression	12/13	25/26
Failure to thrive	3/12	11/20
Hearing loss	6/13	18/26
Generalized or proximal muscle weakness	12/13	25/26
Respiratory insufficiency	8/13	16/23
Non-invasive ventilation	6/13	10/17
Muscular atrophy	12/12	12/12
Myalgia	6/10	6/12
Muscle stiffness	6/12	6/12
Reduced or absent tendon reflexes	12/12	12/12
Calf hypertrophy	4/12	4/12
Joint contractures	7/12	11/23
Progressive scoliosis	7/11	15/21
Waddling gait	4/11	4/11
Broad-based gait	2/11	2/11
Loss of ambulation	6/12	11/25
Elevated creatine kinase	10/10	19/19
Mortality	2/13	2/26

onset muscular dystrophy combined with congenital sensorineural hearing loss and primary ovarian insufficiency in females. All but one affected individual in the report by Foley et al. (2020)² had congenital sensorineural hearing loss, and all 3 postpubertal females had a laboratory-confirmed primary ovarian failure. Andrological examinations on the postpubertal male individuals in the Foley et al. (2020)² report were not available, but none of the 5 male adult individuals has had children. Although a combination of sensorineural hearing loss and muscular dystrophy or myopathy has been described in early-onset facioscapulohumeral dystrophy and Vici syndrome, and an association of early-onset sensorineural hearing loss and primary ovarian insufficiency without muscular dystrophy have been recognized in Perrault syndrome, a constellation of all these three features had not been previously recognized prior to the Foley et al. (2020) study.² Disease course, in particular proximal muscle weakness, was progressive in the series by Foley et al. (2020)² with some interfamilial variability in the rates of deterioration. When comparing the description and course of muscle clinical signs in these previously described affected individuals with expression in the neonatal mouse muscle, there are hints of relatively low *Ggpsi1* expression at this stage compared to the female gonad from E14.5 and we cannot exclude that expression in the muscle increases throughout later development. Muscle histopathology findings in the cohort described by

Foley et al. (2020)² were dystrophic with variable evidence of regenerating fibers, internal nucleation, and core-like regions.

Biallelic pathogenic missense *GGPS1* variants identified in Foley et al. (2020)² have been shown to moderately impair the enzymatic activity of geranylgeranyl diphosphate synthase (GGPPS) (only for 50%) in vitro, and the possible effects of these missense variants on GGPPS function have been speculated to be subtle, putatively including the impairment of the dynamic subcellular localization of the enzyme for cell-type-specific processes, particularly in muscle, ovary, and the inner ear. It had been suggested that the localization of the missense *GGPS1* variants residing outside of the catalytic core of the enzyme could account for the very specific and recognizable clinical phenotype. However, the variants reported in P10 (Family 3) co-locate within the catalytic core of GGPPS and implicate impaired substrate and co-factor binding as potential pathogenic mechanisms, resulting in a phenotype consistent with other reported individuals.

Family 2 in our cohort presents hitherto the largest family (6 affected) with biallelic *GGPS1* variants reported. Affected individuals from our report replicated most of the previously described clinical features associated with *GGPS1* defects. This includes muscular dystrophy with progressive proximal muscle weakness and episodes of variably elevated CK, scoliosis, and respiratory insufficiency. Muscle histopathology findings were also variable but largely consistent with those previously reported by Foley et al. (2020),² including dystrophic changes, regenerating fibers, core-like lesions, internal nucleation, and mitochondrial changes. The lack of dystrophic histopathology and fat infiltration observed in the muscle biopsy and lower limb MRI of Family 3 (P10) may reflect the early age (8 months) at which these investigations were performed, compared to other reported persons. The families described in our report display inter- and intra-familial variability with respect to hearing loss, which was detected only in all affected siblings from Family 1, the probands from Families 3 and 4, and one affected sibling from Family 5. This could suggest that hearing loss might be a variable feature of *GGPS1*-associated muscular dystrophy and is an interesting observation in light of its diffuse expression in the embryonic and postnatal mouse inner ear. Since most of the subjects with unimpaired hearing in the current report were from Family 2, carrying the *GGPS1* c.439A > G, p.(Met147Val) variant, we cannot exclude the possibility of a variant-specific effect. Additionally, our data shows that primary ovarian insufficiency might also be a variable feature of *GGPS1* deficiency, despite strong *Ggpsi1* expression in relevant cells in the embryonic mouse female gonads. Although it is difficult to determine the exact molecular cause of the observed clinical variability, we can

hypothesize a possible link with localisation of the *GGPS1* variants within the gene.

One possible limitation of the present study is the absence of *in vitro* enzyme activity measurements. However, taking into account the findings from the study by Foley *et al.* (2020),² one could expect that the impact of the missense variants from our study on GGPPS function could be subtle as well, with an insignificant reduction of the enzymatic activity of GGPPS. All missense *GGPS1* variants c.269A > G, p.(Asn90Ser), c.439A > G, p.(Met147Val), c.196A > C p.(Ile66Leu), c.545 T > C p.(Leu182Pro) and c.770 T > G p.(Phe257Cys) reported in the current study are ultra-rare across several large genetic databases including 1,314,000 alleles (Table S2) and uniformly predicted to be damaging in various *in silico* prediction tools supporting their disease-causing roles.

Collectively, this report consolidates the disease-causing role of biallelic variants in *GGPS1*, demonstrates that hearing loss and ovarian insufficiency might be variable features of the *GGPS1*-associated muscular dystrophy and implicates impaired substrate and co-factor binding as potential pathogenic mechanisms in this novel form of congenital muscular dystrophy.

Acknowledgements

The authors are grateful to the families for their support and consent to the publication of this study. We acknowledge Kate Michie and Laura Gongolidis for their help with protein modeling.

Conflict of Interest

None of the authors has any conflict of interest to disclose.

Data Availability Statement

The datasets generated during and/or analyzed during the current study are available from the corresponding author on reasonable request.

References

1. Wang M, Casey PJ. Protein prenylation: unique fats make their mark on biology. *Nat Rev Mol Cell Biol.* 2016;17(2):110-122.
2. Foley AR, Zou Y, Dunford JE, *et al.* GGPS1 mutations cause muscular dystrophy/hearing loss/ovarian insufficiency syndrome. *Ann Neurol.* 2020;88(2):332-347.
3. Tucker EJ, Rius R, Jaillard S, *et al.* Genomic sequencing highlights the diverse molecular causes of Perrault syndrome: a peroxisomal disorder (PEX6), metabolic

- disorders (CLPP, GGPS1), and mtDNA maintenance/translation disorders (LARS2, TFAM). *Hum Genet.* 2020;139(10):1325-1343.
4. Makrythanasis P, Maroofian R, Stray-Pedersen A, *et al.* Biallelic variants in KIF14 cause intellectual disability with microcephaly. *Eur J Hum Genet.* 2018;26(3):330-339.
5. Pais LS, Snow H, Weisburd B, *et al.* A web-based analysis and collaboration tool for rare disease genomics. *Hum Mutat.* 2022;43(6):698-707.
6. Natera-de Benito D, Jurgens JA, Yeung A, *et al.* Recessive variants in COL25A1 gene as novel cause of arthrogryposis multiplex congenita with ocular congenital cranial dysinnervation disorder. *Hum Mutat.* 2022;43(4):487-498.
7. Orvis J, Gottfried B, Kancherla J, *et al.* gEAR: gene expression analysis resource portal for community-driven, multi-omic data exploration. *Nat Methods.* 2021;18(8):843-844.
8. Han X, Wang R, Zhou Y, *et al.* Mapping the mouse cell atlas by microwell-seq. *Cell.* 2018;172(5):1091-107.e17.
9. Richards S, Aziz N, Bale S, *et al.* Standards and guidelines for the interpretation of sequence variants: a joint consensus recommendation of the American College of Medical Genetics and Genomics and the Association for Molecular Pathology.
10. Jeong A, Suazo KF, Wood WG, Distefano MD, Li L. Isoprenoids and protein prenylation: implications in the pathogenesis and therapeutic intervention of Alzheimer's disease. *Crit Rev Biochem Mol Biol.* 2018;53(3):279-310.
11. Quinodoz M, Peter VG, Bedoni N, *et al.* AutoMap is a high performance homozygosity mapping tool using next-generation sequencing data. *Nat Commun.* 2021;12(1):518.
12. Kavanagh KL, Dunford JE, Bunkoczi G, Russell RGG, Oppermann U. The crystal structure of human geranylgeranyl pyrophosphate synthase reveals a novel hexameric arrangement and inhibitory product binding. *J Biol Chem.* 2006;281(31):22004-22012.
13. Chang TH, Guo RT, Ko TP, Wang AH, Liang PH. Crystal structure of type-III geranylgeranyl pyrophosphate synthase from *Saccharomyces cerevisiae* and the mechanism of product chain length determination. *J Biol Chem.* 2006;281(21):14991-15000.

Supporting Information

Additional supporting information may be found online in the Supporting Information section at the end of the article.

Figure S1 Region of homozygosity around the variant of interest indicated by a red box.¹¹

Figure S2 3D protein modeling of the *GGPS1* variants in Family 3 (P10).

Figure S3 Expression of *Ggps1* in the mouse cochlea through single-cell RNA-sequencing data.

Figure S4 Expression of *Ggps1* in the mouse embryonic (E14.5) gonad through single-cell RNA-sequencing data.

Figure S5 Expression of *Ggps1* in mouse neonatal leg muscle through single-cell RNA-sequencing data.

Table S1 Extended clinical features of the cases with biallelic *GGPS1* variants.

Table S2 Population frequencies and in silico pathogenicity predictions for *GGPS1* variants reported in this study.

Video S1 Shows P1 with a waddling gait, lower limb weakness, and inverted feet.

Video S2 Shows P4 who is unable to stand unassisted and walk due to the lower limb weakness.

Video S3 Shows P5 with a suggestion of Gower's sign and waddling gait.

Video S4 shows P6 with proximal lower limb weakness.

Video S5 shows P7 with positive Gower's sign.

Video S6 shows P8 with positive Gower's sign.